JCTC Journal of Chemical Theory and Computation

Article

pubs.acs.org/JCTC

Carbon Nanotube Container: Complexes of $C_{50}H_{10}$ with Small Molecules

Helena Dodziuk,*[,†] Tatiana Korona,*[,‡] Enrique Lomba,[§] and Cecilia Bores[§]

[†]Institute of Physical Chemistry, Polish Academy of Sciences, ul. Kasprzaka 44, 01-224 Warsaw, Poland

[‡]Faculty of Chemistry, University of Warsaw, ul. Pasteura 1, 02-093 Warsaw, Poland

[§]IQFR-CSIC, Serrano 119, E-28006, Madrid, Spain

Supporting Information

ABSTRACT: The stability of complexes of a recently synthetized (Scott et al. *J. Am. Chem. Soc.* **2011**, *134*, 107) opened nanocontainer $C_{50}H_{10}$ with several guest molecules, H_2, N_2, CO, HCN, H_2O, CO_2, CS_2, H_2S, C_2H_2, NH_3, CH_4, CH_3CN, CH_3OH, CH_3CCH, 2-butyne, methyl halides, and with noble gas atoms, has been examined by means of symmetry-adapted perturbation theory of intermolecular interactions, which fully incorporates all important energy components, including a difficult dispersion term. All complexes under scrutiny have been found stable for all studied guests at 0 K, but entropic effects cause many of them to dissociate into constituent molecules under standard conditions. The estimation of temperature at which the Gibbs free energy $\Delta G = 0$ revealed that the recently observed (Scott et al. *J. Am. Chem. Soc.* **2011**, *134*, 107) complex $CS_2@C_{50}H_{10}$ is the most stable at room temperature while the corresponding complexes with HCN and Xe guests should decompose at ca. 310 K and that with CO_2 at room temperature (ca. 300 K). In agreement with the ΔG estimation, molecular dynamics simulations performed in vacuum for the $CS_2@C_{50}H_{10}$ complex predicted that the complex is stable but decomposes at ca. 350 K. The MD simulations in $CHCl_3$ solution showed that the presence of solvent stabilizes the $CS_2@C_{50}H_{10}$ complex in comparison to vacuum. Thus, for the complexes obtained in solution the CO_2 gas responsible for the greenhouse effect could be stored in the $C_{50}H_{10}$ nanotube.

INTRODUCTION

In view of energy scarcity and global warming, the application of carbon nanotubes as molecular containers (in particular for H_2 and CO_2) has become a hot topic. As discussed in ref 1, in spite of various claims (see for instance, refs 2 and 3), endohedral fullerenes cannot play this role because, even if a molecule would be inserted into the hydrocarbon, one has to destroy the container cage to recover the guest (however, proposals to derivatize C_{60} in order to induce the reversible formation of C−H bonds[4] or create huge capsules with complicated openings[5] to be used in hydrogen storage should be mentioned). On the other hand, carbon nanotubes (CNTs)[6] opened at, at least, one end would be a natural solution to the problem of extracting the stored molecule. The tubes can be manufactured by several methods, like chemical vapor deposition (CVD),[7] arc discharge[8] or laser ablation[9] methods, and then opened chemically, or alternatively the opened CNTs can be synthesized from scratch. For example, CNT brushes[10] obtained by the CVD method could serve as gas containers.

It should be stressed that a molecular dynamics (MD) study of systems consisting of hydrogen molecules and few model CNTs opened at both ends[11] indicated that, even if hydrogen molecules are stabilized inside the opened containers at low temperatures, most of them leave the tubes at room temperature due to thermal vibrations, resulting in the hydrogen content too low for the CNT applications for hydrogen storage. Of course, the latter results may not be valid for the CNTs opened at one end only.

Noteworthy, prospective nanotube applications are not limited to their use for gas storage. There are also proposals of the CNTs usage as chemical sensors, catalysts, or as electrochemical devices. As a successful example of the first application from the list above one can mention the hydrogen sensor built of carbon nanotubes integrated on a silicon platform, which has been placed on the market by Nanomix Inc. in 2005. There are also patents to use such systems for the detection of carbon dioxide, nitrous oxide, glucose, DNA, etc. A metal-free catalysis of inorganic and organic reactions[12] or selective oxidations[13] is another promising field where the carbon nanotubes can be applied. For instance, oxygen groups attached to the surface of carbon nanotubes have the potential to catalyze oxidative dehydrogenations[14] and nitrogen-doped carbon nanotubes may replace platinum catalysts used to reduce oxygen in fuel cells. A "forest" of vertically aligned nanotubes, that is a CNT brush, can reduce oxygen in alkaline solution more effectively than platinum, which has been used in such applications since the 1960s. Here, the nanotubes have the added benefit of not being subjected to carbon monoxide poisoning. Another exciting field of application of opened fullerenes (i.e., short CNTs opened at one end), with or without a guest, is in the domain of electrochemical switching devices. Itaya et al.[15] achieved a 1:1 supramolecular assembled film of an opened-cage fullerene and zinc(II)-octaethylporphyrin on an Au(111) surface with the porphyrin sitting on the surface and the cages on top of them with openings orientated toward the solution. Such films formed on

Received: June 28, 2012
Published: September 13, 2012

   dx.doi.org/10.1021/ct300546c | *J. Chem. Theory Comput.* 2012, 8, 4546−4555

the surface are characterized by a well-defined chemical response.

Very recently, Scott et al. published a synthesis of a $C_{50}H_{10}$ nanotube opened at one end and found that it forms a stable complex with CS_2 inside (Figure 1).[16] To our best knowledge,

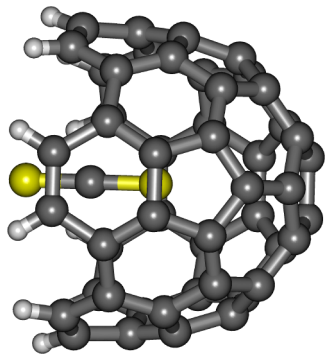

Figure 1. $CS_2@C_{50}H_{10}$ complex.

it is the first complexation report with a synthesized nanotube host, not counting few such studies for opened C_{60} and C_{70} derivatives summarized in refs 17 and 18. In continuation of our former studies of small molecular guests in intact fullerenes C_{60} and C_{70}, symmetry-adapted perturbation theory (SAPT)[19−21] is applied to the complexes of the $C_{50}H_{10}$ nanotube with the following guests: H_2, N_2, CO, HCN, H_2O, CO_2, CS_2, H_2S, C_2H_2, NH_3, CH_4, CH_3CN, CH_3OH, CH_3CCH, 2-butyne, methyl halides, and with noble gas atoms. In addition to complexation energies, free energies of complexation are estimated for several complexes and some molecular dynamics calculations for the complex $CS_2@C_{50}H_{10}$, which was experimentally found stable,[16] are reported. Our results indicate that carbon nanotubes could be used as nanocontainers for the CO_2 gas responsible for the greenhouse effect. They can also be useful for designing future experiments involving the $C_{50}H_{10}$ compound and similar species.

METHODS

The stability of a complex consisting of a molecule A residing at least partly inside the cage of a molecule B (A@B) can be examined by the same methods as any other noncovalent (van der Waals) complex. The complex is stable at some finite temperature and pressure, if the Gibbs free energy of the encapsulation reaction (A + B → A@B) is less than zero, $\Delta G(T) < 0$. This energy can be obtained as the sum of internal energy, which in our case is the stabilization energy, and the Gibbs thermal correction. The first term, i.e. the stabilization energy is the interaction energy of A@B at the minimum of the potential energy surface (PES),

$$E_{\mathrm{int}} = E(\mathrm{A@B}) - [E(\mathrm{A}) + E(\mathrm{B})] \quad (1)$$

The reliable calculation of this energy is a difficult task, since the dispersion interactions for the large electron-rich $C_{50}H_{10}$ host are expected to play a significant role in the stabilization of the complex. Therefore, a proper computational method should be used to estimate the long-range electron correlation effects accurately enough. Among theoretical methods for the E_{int} calculations, the supermolecular methods with electronic energies obtained with e.g. Møller−Plesset theory to the second order, MP2, or with density-functional theory (DFT) are usually used. However, both MP2 and DFT have their drawbacks, which have prevented us from applying them. The MP2 method is known to overestimate interactions for stacked complexes[22] (the same effect was also observed for $Rg@C_{60}$ species),[23] while DFT with currently utilized functionals fails to describe the long-range electron correlation correctly and cannot be used with confidence for noncovalent interactions. As a practical cure for the DFT drawbacks, a so-called empirical dispersion correction was recently proposed[24,25] while a spin-component-scaled MP2 method (SCS-MP2)[26] has been shown to improve the behavior of MP2 in many cases. However, both approaches, DFT+Disp and SCS-MP2, contain some adjustable parameters making them less reliable than pure ab initio methods. In this work, we use a perturbational alternative to obtain the interaction energy, denoted as symmetry-adapted perturbation theory (see refs 19−21 for reviews). In SAPT, the interaction energy up to the second order in terms of the unexpanded intermolecular potential V is defined as a sum of three Rayleigh−Schrödinger corrections: first-order electrostatic ($E^{(1)}_{\mathrm{elst}}$), second-order induction ($E^{(2)}_{\mathrm{ind}}$), and second-order dispersion ($E^{(2)}_{\mathrm{disp}}$) energies, and their exchange counterparts, accounting for electron tunneling between A and B, namely, first-order exchange ($E^{(1)}_{\mathrm{exch}}$), second-order exchange-induction ($E^{(2)}_{\mathrm{exch\text{-}ind}}$), and second-order exchange-dispersion ($E^{(2)}_{\mathrm{exch\text{-}disp}}$) energies.

Higher-order (in V) induction and exchange-induction effects are usually estimated by the δE_{HF} term.[27,28] This term is obtained as a difference between the supermolecular Hartree−Fock (HF) interaction energy and a sum of electrostatic, first-order exchange, second-order induction, and exchange-induction components calculated from the HF monomers. The electron correlation inside the interacting molecules can be accounted for on various levels of theory (note that—untypically to other perturbational theories—no exact eigenvalues and eigenvectors of the zeroth-order Hamiltonian are available), like the Hartree−Fock (no electron correlation), MP, coupled cluster, or DFT levels. For large molecules, only HF and DFT can be used for obvious reasons, making the SAPT(DFT) method the only SAPT-type method capable to treat large molecules with inclusion of intramolecular electron correlation. It should be emphasized that in SAPT(DFT) the difficult long-range electron correlation (between interacting molecules) is taken into account by perturbational theory, while the short-range electron correlation (inside interacting molecules) is treated by DFT.[29−37] Nowadays, the implementation of SAPT(DFT), followed by the utilization of the density fitting (DF) approximation[38] to electron-repulsion integrals,[39−42] allows us to use SAPT for large van der Waals molecules, like dimers of cyclotrimethylene trinitramine,[43] complexes of water with circumcoronene,[44] or for endohedral complexes of fullerenes,[17,23,45,46] studying DNA-intercalator interactions,[47] or the vancomycin complex with a diacetyl-Lys-s-Ala-d-Ala bacterial wall precursor.[46] The accuracy of SAPT(DFT) was verified by comparisons with the CCSD(T) calculations[39,41] and by the benchmark SAPT(CCSD) studies.[48−54] SAPT(DFT) still scales with the fifth power of the molecular size because of a high cost of the dispersion and exchange-dispersion components, so it is impossible to calculate the whole SAPT(DFT) intermolecular potential energy surface or to perform a geometry optimization for $X@C_{50}H_{10}$ complexes. Therefore other, more approximate, methods have to be used for this purpose. To this end, we utilized molecular mechanics (MM)[55,56] to obtain stationary-point geometries for complexes of $C_{50}H_{10}$ with all molecules.

dx.doi.org/10.1021/ct300546c | J. Chem. Theory Comput. 2012, 8, 4546−4555

Our experience with the MM optimizations suggests that for endohedral complexes with nonpolar or slightly polar guests it gives quite reliable geometries, what can be explained by an empirical inclusion of important components of the interaction energy into the MM parametrization. In particular, in this aspect MM is often superior over DFT geometries, being at the same time much cheaper (an average DFT optimization with the subsequent frequencies calculation may take more than a week to complete on the Intel-Xeon with CPU E54020@2.50 GHz) (serial calculations). However, it is impossible to use MM for the complexes with noble gases, so in these cases the DFT optimized geometry was used. The obtained stationary points are local minima for a selected method (all harmonic frequencies were positive), but they will be of course a bit different for various approaches. In particular, the DFT geometry optimization of $Rg@C_{50}H_{10}$ might put the Rg atom in a larger distance from the $C_{50}H_{10}$ center of mass because of the lack of a proper description of dispersion in DFT. However, recent results for the $H_2@C_{60}$[45] and for $Rg@C_{60}$[23] complexes show that the potential energy surface is rather flat in the vicinity of the minimum, and that small shifts from the optimal position of the guest do not change stability predictions of the complex. This flatness of the PES results from the behavior of the dominant dispersion and first-order exchange contributions (which behaves like const + $O(r^2)$),[23,57] where r is the distance of the guest from the C_{60} center). This feature can be expected to persist for the present case.

In order to obtain the Gibbs free energy $\Delta G(T)$ for the encapsulation reaction in the gas phase, we need to add the Gibbs thermal correction ($\Delta g(T)$) to the electronic energy E_{int} calculated for the minimum geometry of the complex. If usual approximations for the calculations of this term are utilized, i.e. the ideal gas assumption, the separation of rotations and vibrations, the rigid-rotor approximation for rotations and the harmonic approximation for vibrations, this correction comprises the translational and rotational terms plus the PV term, which give together a contribution of $-n/2\ RT$ (n = 5, 7, 8 for atomic, linear, and nonlinear guests, respectively), the zero-point vibrational energy (ΔZPVE), the thermal vibrational correction ($\Delta u(T)$), and the entropic contribution ($-T\Delta S(T)$).

$$\Delta G(T) = E_{int} + \Delta g(T) \quad (2)$$

$$\Delta g(T) = \Delta ZPVE + \Delta u(T) - n/2RT - T\Delta S(T) \quad (3)$$

We are aware that for floppy and weakly interacting molecules such approximations may bear significant errors, which should be kept in mind when analyzing the results. However, the similar conclusions concerning the temperature stability for the $CS_2@C_{50}H_{10}$ complex provided by the MD simulations gives us some confidence in the validity of our results also for other $C_{50}H_{10}$ guests. It should be noted that energetically equivalent minima resulting from the symmetry of molecules under study are automatically accounted for in the entropic contribution through the rotational constants. Additionally, both minima "out" and "in" for the complex with the carbon monoxide molecule were treated as equivalent ones, since they were very close energetically and were easily accessible through the rotation because of a very low barrier. From all terms given in eq 3, the vibrational contributions are the most cumbersome to calculate. A usual way to obtain this part of $\Delta g(T)$ consists in calculating separately the corresponding contributions at a given temperature for all three systems A@B, A, and B and by making a subtraction, analogously to eq 1. Unfortunately, this procedure is not accurate enough if the MM frequencies are used, because here two very similar numbers for A@B and A+B are subtracted from each other and frequencies obtained from the MM optimizations contain too large numerical errors. Apart from this accuracy problem, the procedure of obtaining a temperature dependence of $\Delta G(T)$ would require an explicit consideration of over a hundred harmonic vibrational modes for $X@C_{50}H_{10}$ and $C_{50}H_{10}$ in the vibrational part of the partition function. Therefore, in order to estimate these contributions, we adopted a different approach, which is based on analyzing the low frequencies of the $X@C_{50}H_{10}$ complexes and selecting those corresponding to the translation and rotation of the whole guest with respect to the cage, i.e. we assume that inter- and intramolecular vibration can be separated. The former frequencies (3, 5, or 6 for atomic, linear, or nonlinear guest molecule, respectively) are then used to calculate the vibrational frequencies directly using common textbook formulas (see, e.g., ref 58 for a comprehensive introduction to this topic). The selected vibrational frequencies are given in the Supporting Information.

We checked that this procedure works well for atomic and rigid-molecule guests for the B3LYP vibrational frequencies (differences between $\Delta G(T)$ values obtained by the standard and the present approach do not exceed 1.2 kcal/mol). (Note parenthetically that proper care should be taken to correctly account for the rotational symmetry number of a molecule[59,60] for the rotational entropic contribution.)

The final part of our calculation was the MD simulations for the complex of CS_2 with $C_{50}H_{10}$, observed by Scott et al.[16] Simulations of the latter system have been performed using the LAMMPS code,[61−64] both in vacuum and in the presence of $CHCl_3$ as solvent in the canonical ensemble. Additionally we have obtained estimates of the ligand Gibbs free energy using targeted molecular dynamics (TMD)[65] calculations as implemented in the LAMMPS code as well.[61−64] Carbon and hydrogen atoms at the nanotube end interact by means of an adaptative intermolecular reactive empirical bond order potential,[66,67] which has been shown to perform effectively in the simulations of single-wall and multiwalled carbon nanotubes.[68,69] Additionally, for the CS_2···nanotube interaction we have used the potential model of Kholmurodov et al.,[70] with parameters for the CS_2 taken from the work of Zhu et al.[71] including intramolecular contributions (i.e. stemming from vibrations of the CS_2 molecule). The partial charges for CS_2 and $C_{50}H_{10}$ were obtained from the natural bond orbital analysis, as implemented in MOLPRO[72,73] from the PBE[74] one-electron densities. These factors must be taken into account due to the presence of a significant quadrupole moment in the CS_2 molecule. Finally, the intermolecular C···H interaction is taken from the work of Phillips and Hammerbacher,[75] and the potential model for chloroform follows the work of Benjamin.[76] This model also accounts for intramolecular vibrations, and quantitatively agrees with the spectroscopic data. Cross-interactions are defined in terms of the Lorentz−Berthelot rules.[77]

Using this potential model for the $CS_2@C_{50}H_{10}$ system, we have calculated the potential energy profile along the main symmetry axis of the nanotube, shifting the position of CS_2 along the symmetry axis. When the solvent is added, the simulations have been started from an initial configuration using 2048 molecules of $CHCl_3$ in a cubic box of the side length of 64.86 Å, so as to reproduce the experimental density

Table 1. SAPT Components of the Interaction Energy (kcal/mol) for the Complexes of $C_{50}H_{10}$ with Guest Molecules at Minimum Geometries

guest	$E^{(1)}_{elst}$	$E^{(1)}_{exch}$	$E^{(2)}_{ind}$	$E^{(2)}_{exch\text{-}ind}$	$E^{(2)}_{disp}$	$E^{(2)}_{exch\text{-}disp}$	δE_{HF}	E_{int}
H_2	−1.31	3.93	−0.96	0.86	−6.07	0.72	−0.13	−2.96
N_2	−3.72	10.39	−3.43	3.28	−14.32	1.59	−0.70	−6.90
CO (in)	−4.52	11.49	−4.39	4.14	−15.18	1.91	−0.68	−7.22
CO (out)	−4.08	11.19	−3.61	3.40	−15.09	1.76	−0.75	−7.18
HCN (in)	−6.57	14.50	−6.44	5.21	−18.57	2.61	−0.93	−10.19
HCN (out)	−3.14	12.53	−5.55	4.27	−16.29	2.15	−0.83	−6.87
H_2O	−2.84	8.64	−4.23	2.83	−11.96	1.66	−0.30	−6.20
CO_2	−5.66	12.43	−5.32	4.84	−17.52	1.94	−0.50	−9.79
CS_2	−17.33	42.02	−26.15	25.45	−41.71	7.62	−1.85	−12.36
H_2S	−11.48	29.21	−16.94	15.84	−26.30	5.15	−0.94	−5.46
C_2H_2	−6.83	20.38	−9.83	9.14	−23.34	3.95	−0.80	−7.32
NH_3	−6.50	16.01	−8.82	7.48	−17.26	3.00	−0.52	−6.61
CH_4	−6.67	19.81	−6.24	6.03	−18.14	2.92	−0.99	−3.28
CH_3CN (in)	−8.88	21.17	−10.42	8.42	−25.58	3.70	−1.17	−12.76
CH_3CN (out)	−10.78	31.85	−12.81	10.53	−31.73	4.76	−2.00	−10.17
CH_3OH (in)	−6.26	17.94	−6.91	5.78	−19.60	2.73	−1.22	−7.54
CH_3OH (out)	−8.34	23.94	−9.45	8.41	−23.07	3.61	−1.44	−6.32
CH_3C_2H (in)	−7.87	23.06	−12.05	11.34	−27.98	4.56	−0.94	−9.89
CH_3C_2H (out)	−8.86	24.19	−9.06	8.24	−25.68	3.86	−1.62	−8.94
$CH_3C_2CH_3$	−8.34	27.06	−10.90	9.98	−30.82	4.73	−1.61	−9.90
CH_3F (in)	−6.51	15.69	−4.89	4.11	−18.34	2.28	−0.87	−8.52
CH_3F (out)	−7.70	22.45	−8.63	7.99	−19.85	3.02	−1.47	−4.19
CH_3Cl (in)	−8.36	21.07	−10.33	9.67	−24.34	3.75	−0.83	−9.37
CH_3Cl (out)	−6.81	17.30	−7.00	6.28	−19.36	2.60	−1.17	−8.16
CH_3Br (in)	−14.35	34.27	−22.08	21.21	−33.90	6.32	−1.14	−9.67
CH_3Br (out)	−7.37	18.78	−8.44	7.59	−21.73	2.91	−1.26	−9.52
CH_3I (in)	−13.76	26.72	−23.71	21.06	−31.56	5.93	0.42	−14.90
CH_3I (out)	−8.46	20.55	−10.68	8.72	−24.32	3.32	0.00	−10.87
He	−0.57	2.45	−0.20	0.19	−3.07	0.20	−0.16	−1.14
Ne	−1.89	5.98	−2.41	2.61	−6.60	0.68	−0.20	−1.83
Ar	−4.01	11.12	−4.78	4.65	−15.20	1.84	−0.41	−6.79
Kr	−11.41	26.52	−16.96	15.46	−27.61	4.73	1.03	−8.23
Xe	−17.43	38.47	−30.10	26.23	−35.72	7.03	2.80	−8.72

at room temperature (1.48 g/cm^3). From this configuration, 16 molecules are removed to insert $CS_2@C_{50}H_{10}$, and the resulting system is equilibrated using temperature rescaling for 10 ps. Then, simulations were run at 220 (just above the solvent's melting temperature), 260, 298, and 360 K. The latter temperature is slightly above the boiling temperature of the solvent (∼335 K), and since in our case we have run the simulation in a canonical ensemble, it corresponds to an overheated liquid (i.e., a metastable state), which has been only considered with the purpose of testing the thermal stability of the complex in the presence of a solvent. A time-step of 1 fs has been used during the simulations (no substantial difference was found in the results using a 0.5 fs time-step). The equilibration runs were 10 ps long in a microcanonical ensemble using temperature rescaling every 500 time-steps. Subsequently, temperature was fixed using a Hoover thermostat,[77] and production runs were 1 ns long. In order to assess the effect of the solvent, we have also run simulations in vacuum at 300 and 350 K, with temperature rescaling every 200 steps in order to keep the temperature at the desired value. Given the small number of atoms involved, the use of a thermostat is inefficient, and even with rescaling, deviations sometimes larger than 20% can be observed. Finally, making use of the TMD approach,[65] we have obtained a more quantitative assessment, approximating the Gibbs free energy as the work required to remove the CS_2 molecule from the nanotube container. To that purpose, TMD simulations have been run for the complex $CS_2@C_{50}H_{10}$ in vacuum at T = 0.1 K and at T = 298 K for 4 ns and in the presence of chloroform as solvent at 298 K for 1 ns. We have used a distance type reaction coordinate, ρ, that measures the root-mean-square displacement of the CS_2 molecule from the equilibrium position inside the host and the molecular dynamics is driven according to the prescription of ref 65 until the value of ρ indicates that the guest is well off the host. In the case of simulations in the presence of solvent, we have also run simulations removing the host−guest interactions in order to obtain reference results that illustrate the effect of the solvent on the bare CS_2 molecule.

■ COMPUTATIONAL DETAILS

The geometry optimizations for most complexes were performed with help of the MM method with the universal force field (UFF).[78,79] All obtained stationary points are local minima (all harmonic frequencies are positive, as verified by the UFF implementation in Gaussian 03).[80] For $Rg@C_{50}H_{10}$ complexes, as well as for selected complexes of $C_{50}H_{10}$ with other guests, the DFT optimization was additionally performed. In this case, the standard B3LYP functional[81−83] in the 6-31G(d) basis set (3-21G for xenon)[84] was utilized. All these optimizations were performed by Gaussian03.[80]

dx.doi.org/10.1021/ct300546c | J. Chem. Theory Comput. 2012, 8, 4546−4555

The SAPT(DFT) interaction energies were obtained with the MOLPRO suite of codes[85] at MM optimized geometries (with the exception of Rg@$C_{50}H_{10}$, see above). For a description of the electron correlation in monomers within the SAPT(DFT) method, the PBE[74] functional with an asymptotic correction of Grüning et al.[86] has been used. Ionization potentials needed for the calculation of the asymptotic corrections have been either obtained from ref 87 or calculated as a difference of the unrestricted Kohn−Sham (KS) energy for the guest molecule with one electron removed and the restricted KS energy for a neutral molecule (for the $C_{50}H_{10}$ host). The def2-TZVP basis[88,89] has been used for all but Rg atoms, for which the aug-cc-pVTZ basis[90,91] (He, Ne, Ar) or the aug-cc-pwCVTZ-PP basis[92] (Kr, Xe) was utilized. Note that the latter basis indirectly includes relativistic effects for the core electrons. For the iodine atom, the effective core potential (ECP) of the ECP28MDF type[93] was used. It has been shown previously that a similar basis gives quantitatively good results at a still affordable computational time for endohedral fullerene complexes.[45] Additionally, for the CS_2@$C_{50}H_{10}$ species one SAPT(DFT) calculation using the def2-QZVP basis has been performed. Since this calculation took about 16 days instead of the 3.5 days needed for the one with the smaller basis, it was not repeated for other complexes. For the DF version of SAPT(DFT), the special auxiliary basis sets are also needed. These basis sets were taken from refs 90 and 94 for almost all atoms with the exception of krypton and xenon, where the def2-QZVPP/JKFIT basis was utilized,[95] and the helium atom, for which an even-tempered basis described in ref 23 was used. Core electrons (1s for C, N, O, F, Ne, 1s2s2p for Cl, S, Ar, 1s2s2p3s3p3d for Br, and the lowest 4 remaining orbitals for I) were frozen in electron-correlated calculations. The ionization potentials and HOMO energies used in SAPT(DFT) calculations are collected in the Supporting Information.

Harmonic frequencies from the geometry optimization of X@$C_{50}H_{10}$ were selected according to the amplitudes of the guest atoms for a given mode, so that they correspond to the translational-rotational modes of the guest inside the cage. In several cases the necessary number of low frequencies cannot be selected unambiguously. Such situations occur for larger and/or floppy guests (like methane and its derivatives), and such complexes were excluded from the free energy analysis.

RESULTS AND DISCUSSION

SAPT and Gibbs Free Energy Results. The models of minimized structures of all complexes under study, ionization potentials (IP) and HOMO PBE energies used for the SAPT(DFT) calculations as well as intermolecular guest−host vibrations are presented in the Supporting Information. The total interaction energy and its components for all complexes under study are presented in Table 1 while zero-point vibrational energies ΔZPVE, vibrational thermal corrections, free Gibbs energy for standard conditions for the encapsulation reaction X + $C_{50}H_{10}$ → X@$C_{50}H_{10}$, and the estimated temperature $T_{\Delta G=0}$, for which the complex X@$C_{50}H_{10}$ becomes thermodynamically stable at 1 atm are collected in Table 2. For nonsymmetrical molecules, two orientations of a guest inside the cage were taken into account. For molecules with the methyl group one such orientation has been denoted as "out", if the methyl group is inside the hole, while the reverse orientation has been called "in". For hydrogen cyanide and carbon monoxide, the "in" orientation has the nitrogen or carbon atom, respectively, in the $C_{50}H_{10}$ hole. All values of interaction energies E_{int} collected in Table 1 are negative, showing that each complex is stabilized in comparison to the isolated host and guest. This effect results from several factors. $E^{(1)}_{elst}$, $E^{(2)}_{ind}$, and $E^{(2)}_{disp}$ are negative and exert stabilizing effect while positive $E^{(1)}_{exch}$, $E^{(2)}_{exch\text{-}ind}$, and $E^{(2)}_{exch\text{-}disp}$ terms act in the opposite direction. Noteworthy, δE_{HF} values are usually small and negative (mostly less than 1 kcal/mol in absolute value) for all but CH_3I *in* and *out*, Kr, and Xe. The large in absolute value dispersion contribution in the SAPT interaction energy represents an additional stabilization effect which is absent in the HF and partially absent in the DFT supermolecular interaction energies. Except for Xe, CH_3I in and out, CH_3CN out, and H_2O guests, for all other complexes under investigation the $E^{(2)}_{ind}$ and $E^{(2)}_{exch\text{-}ind}$ terms have close absolute values and almost cancel. Such a behavior is typical for interacting nonpolar or weakly polar molecules, as well as in the PES regions with substantial electron cloud overlaps. Even for molecules with a nonzero dipole or quadrupole moment, like water, HCN, or CS_2, the net contribution of these two

Table 2. Zero-point Vibrational Energies ΔZPVE, Free Gibbs Energy for Standard Conditions for the Encapsulation Reaction X + $C_{50}H_{10}$ → X@$C_{50}H_{10}$ (kcal/mol), Thermal Vibrational Correction $\Delta u(298.15)$, and the Estimated Temperature $T_{\Delta G=0}$ (Kelvin) for Which the Complex X@$C_{50}H_{10}$ Becomes Thermodynamically Stable at 1 atm Together with the Interaction Energy E_{int} for Selected Complexes from Table 1[a]

guest	E_{int}	ΔZPVE	$\Delta G(298.15)$	$\Delta u(298.15)$	$T_{\Delta G=0}$
H_2	−2.96	0.87	1.37	2.20	180
N_2	−6.90	0.64	2.09	2.37	220
CO	−7.22	0.68	1.75	2.35	230
HCN (in)	−10.19	0.72	−0.30	2.30	310
H_2O	−6.20	1.10	1.98	1.10	210
CO_2	−9.79	0.54	−0.01	2.46	300
CS_2	−12.36	0.59	−1.50	2.43	340
		(0.37)	(−1.54)		
H_2S	−5.46	1.10	3.70	2.59	160
C_2H_2	−7.32	0.88	2.80	2.18	210
		(0.40)	(1.63)		
NH_3	−6.61	1.08	1.72	2.60	230
CH_4	−3.28				
		(1.26)	(4.70)		
CH_3C_2H (in)	−9.89	0.85	0.31	2.79	290
CH_3Br (in)	−9.67	0.76	0.44	2.87	280
		0.09	(1.52)		
He	−1.14	0.60	4.70	1.25	40
		0.66	(6.72)		
Ne	−1.83	0.25	3.69	1.54	90
		0.04	(5.33)		
Ar	−6.79	0.32	0.56	1.48	270
		(0.30)	(0.69)		
Kr	−8.23	0.33	0.03	1.47	300
		(0.09)	(−0.06)		
Xe	−8.72	0.31	−0.32	1.49	310
		(0.08)	(−0.18)		

[a]Geometries of the type in (as always corresponding to the lower energy) except for CO were used. In parentheses $\Delta G(298.15)$ obtained from DFT B3LYP optimizations of complex and constituent molecules (atoms) (plus the SAPT(DFT) interaction energy from Table 1) are given, if available.

dx.doi.org/10.1021/ct300546c | J. Chem. Theory Comput. 2012, 8, 4546−4555

components is quite small in comparison to the total energy. The stability at 0 K of all nanotube complexes under study is very different from that in endohedral fullerene cases[17,45] where destabilization was predicted for several larger molecules. This difference can be easily explained by the fact that for the opened cage the guest does not have to be completely inserted inside the hole, resulting in a reduction of the valence (Pauli) repulsion $E^{(1)}_{exch}$ between the host and the guest.

For all complexes under study, the out orientation is less stable than the in one. For CO and CH_3Br guests, the differences in E_{int} energy are very small (0.04 and 0.15 kcal/mol) while the corresponding values for CH_3F, CH_3I and HCN are considerably larger (4.41 kcal/mol, 4.03 and 3.32 kcal/mol, respectively). These differences cannot be attributed to a specific factor in view of a subtle interplay among dispersion, exchange, electrostatic, and other contributions to E_{int}. The second-order stabilizing dispersion term $E^{(2)}_{disp}$ is, in the absolute value, the largest, except for 8 out of 33 complexes under investigation (involving CS_2, H_2S, CH_4, CH_3CN in, CH_3OH out, CH_3F out, CH_3Br in, and Xe guests); otherwise, the $E^{(1)}_{exch}$ destabilizing term is the largest resulting in the dispersion term being the second one in the absolute value. A dominant role of the dispersion term is understandable since the guest atoms are situated at a favorable distance (close to the van der Waals minima) to the host $C_{50}H_{10}$ nanotube. In most cases, $E^{(1)}_{elst}$, $E^{(2)}_{ind}$, and $E^{(2)}_{exch\text{-}ind}$ have similar values while those of $E^{(2)}_{exch\text{-}disp}$ are (except for the He guest) the smallest.

For the noble gas complexes all consecutive corrections grow in an absolute value steadily with the increasing guest atom, but the final interaction energy results from a delicate balance between all contributions, leading to an unexpected small difference in stabilization energy for the complexes with He and Ne guests. It should be noted however that these results come from a single-point calculations for the DFT minima of both species, and it is probable that a true minimum of Ne@$C_{50}H_{10}$ lies for the neon atom closer to the center (the DFT method does not take into account correctly stabilizing dispersion while at the same time Ne undergoes a stronger repulsion from $C_{50}H_{10}$ than a smaller helium atom). Since we are aware that the utilized def2-TZVP basis is only of a moderate quality, we tested how the energy changes for the same geometry when the larger def2-QZVP basis is used for the CS_2@$C_{50}H_{10}$ complex. Similarly to previous findings,[45] most SAPT components are already saturated in the smaller basis, but the second-order dispersion becomes larger (in the absolute value) by 2.3 kcal/mol. In total the interaction energy is lowered by 2.0 kcal/mol, i.e. by ca. 15%, when the better def2-QZVP basis was used. Similar results should be expected for other complexes, too, so the true stabilization energies will be always lower by a couple of kilocalories per mole than the results from Table 1.

The E_{int} values providing an estimation of the enthalpy of the complex formation (without the ZPVE correction) showed that all complexes under study were stabilized at 0 K. However, to draw conclusions concerning the observation of the complexes under scrutiny at room temperature, the free Gibbs energy for standard conditions for the encapsulation reaction X + $C_{50}H_{10}$ → X@$C_{50}H_{10}$, ΔG and the temperature $T_{\Delta G=0}$ at which the complex X@$C_{50}H_{10}$ becomes thermodynamically stable at 1 atm should be estimated. In Table 2 interaction energy E_{int}, zero-point vibrational energies ΔZPVE, ΔG, $\Delta u(T)$, and the estimated temperature $T_{\Delta G=0}$ rounded to 10 K for selected complexes from Table 1 are listed. As explained in the Methods section, for several large and/or floppy molecules, the unambiguous selection of the interhost−guest vibrational modes was not possible. Thus, for some of these molecules additionally the DFT optimization was performed and the minimum was found. For these complexes, one can calculate a thermal correction to ΔG as a difference between the values for A@B, A, and B and use it instead of the quantity obtained from a direct use of n vibrational modes. Such values are given in parentheses in Table 2. Noteworthy, for cases where both approaches were used, ΔG at T = 298.15 K have very close values, showing that the direct method of including vibrational contributions provided reliable estimation of this quantity.

The values collected in Table 2 show that for most complexes the Gibbs free energy of the encapsulation reaction becomes positive and they become unstable at standard conditions. The $T_{\Delta G=0}$ data indicate that only few complexes should be possible to observe. Remarkably, in agreement with the experimental finding,[16] the highest $T_{\Delta G=0}$ value was found for the CS_2 guest. The HCN, Xe, and possibly CO_2, Kr, and CH_3C_2H were other candidates for a successful complexation. If the influence of solvent is taken into account (see below the results of MD simulations for the complex involving CS_2), then the CO_2 gas, responsible for the greenhouse effect, could be stored in the nanotube under scrutiny. On the other hand, $C_{50}H_{10}$ cannot be used as the H_2 container since already at 180 K the H_2@$C_{50}H_{10}$ complex becomes unstable. Although E_{int} for this complex has a negative value, the major destabilizing contribution, the entropic term, grows quickly with temperature. According to the $\Delta G(T)$ analysis, the CS_2@$C_{50}H_{10}$ complex detected by Scott et al.[16] is stable at room temperature but decomposes if the temperature is increased by about 50 K. Its lighter analog involving CO_2 becomes unstable at 300 K, but taking into account the stabilizing effect of the $CHCl_3$ solvent on the CS_2@$C_{50}H_{10}$ complex (see the MD simulations), the nanotube application as a nanocontainer for the latter gas seems feasible. For the case of CO@$C_{50}H_{10}$, in and out conformations are very close energetically (by 0.04 kcal/mol; see Table 1). Thus, in this case the equal probability of the two minima was assumed, resulting in an additional entropic term of $-RT$ ln 2 in the Gibbs energy. Inclusion of the latter term did not change considerably the conclusion concerning stability of the CO@$C_{50}H_{10}$ complex. For the CH_3Br@$C_{50}H_{10}$ complex, the in and out cases are also quite close in energy (0.15 kcal/mol). However, in this case a higher barrier between those minima is expected in view of high steric repulsion of electron-rich CH_3Br guest and the $C_{50}H_{10}$ nanotube. Therefore, the in and out cases were treated as different isomers. It should be noted that these conclusions are valid under assumption that reagents and products are present in the gas phase. Other techniques should be necessary to evaluate the stability in solution. For the carbon disulfide molecule, we performed such an analysis by means of MD (see the section on Molecular Dynamic Simulations).

Noteworthy, the increase of pressure above atmospheric pressure can also be used to stabilize the complexes and to obtain a measurable yield of filled $C_{50}H_{10}$ molecules.

Molecular Dynamics Simulations. Using the empirical potential model for the CS_2@$C_{50}H_{10}$ complex, we have calculated the potential energy profile along the main symmetry axis of the nanotube, shifting the position of the CS_2 along the symmetry axis. This is depicted in Figure 2, where the binding energy of the latter molecule in the nanotube is plotted with respect to the separation of guest carbon atom and the

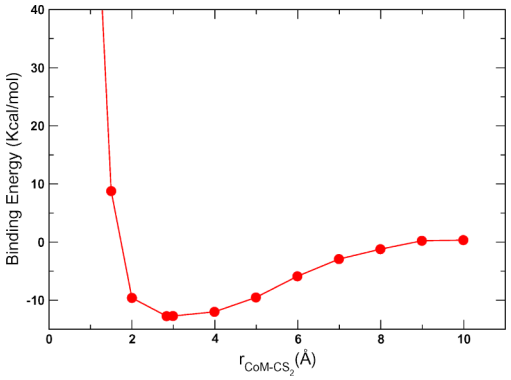

Figure 2. Binding energy of the CS_2 molecule (lying inside the nanotube along its principal symmetry axis) at 0 K as a function of the separation between the centers of mass of the guest molecule and of the nanotube determined from the effective potentials used in the MD calculation.

nanotube center of mass. An energy minimum of −12.7 kcal/mol at about 3 Å separation between the CS_2 and the nanotube centers of mass shown indicates that the guest molecule should have a definite tendency to remain inside the nanocage. This minimum is in a very good agreement with the SAPT(DFT) result from Table 1 (of −12.36 kcal/mol) and corresponds exactly to the binding energy obtained from our empirical potential model when minimizing the corresponding potential energy for both the host−guest system and the two separate components. The thermal stability of the host−guest system in vacuum is depicted in Figure 3. Here one observes that the

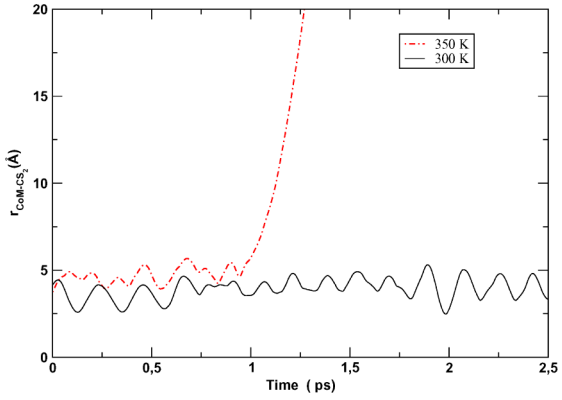

Figure 3. Temperature dependence of the relative position of the CS_2 molecule with respect to the nanotube center of mass determined by the MD run for the $CS_2@C_{50}H_{10}$ complex in vacuum.

guest molecule remains in the cage at 300 K at a distance of 3.5 Å of the cage's center of mass, but for higher temperatures, it leaves the cage, despite the relatively high dissociation energy. This can be understood as the result of the thermal fluctuations modifying the configuration of the guest (due to rotations and vibrations) and also to the changes in the potential energy landscape of the host due to vibrations of the nanotube. Note that this is a pure enthalpic analysis, and entropic effects have been so far neglected. When the solvent is added, the situation is drastically modified (Figure 4). Now the equilibrium position of the CS_2 molecule moves slightly in the direction of the nanotube opening, due to the attractive interaction exerted by the solvent on the guest molecule.

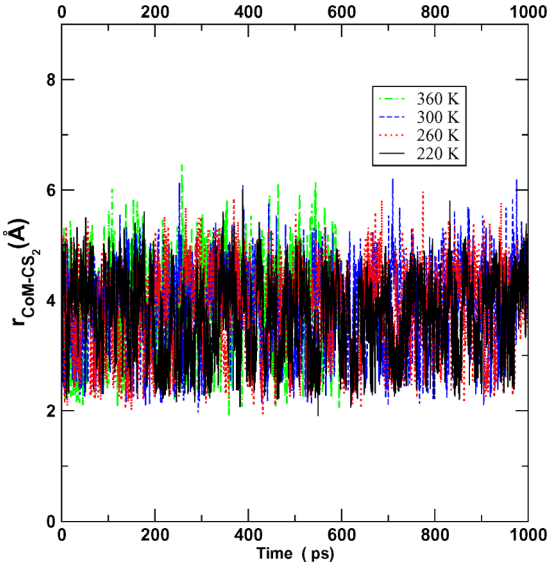

Figure 4. Temperature dependence of the relative position of the CS_2 molecule with respect to the nanotube center of mass determined by the MD run for the complex $CS_2@C_{50}H_{10}$ in chloroform.

However, the net effect of the solvent is the complex stabilization. These trends are presented in Figure 5 showing

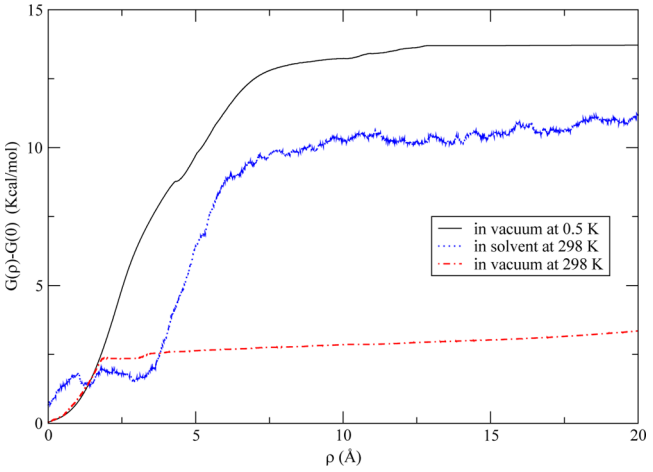

Figure 5. Temperature dependence of the work required to remove the CS_2 molecule from the $CS_2@C_{50}H_{10}$ complex, in vacuum at 0.5 and 298 K and in the presence $CHCl_3$ at 298 K, in terms of the ρ reaction coordinate.

the results of TMD calculations. Here the work needed to remove the CS_2 molecule from the $CS_2@C_{50}H_{10}$ complex at constant pressure is depicted in vacuum and in the solution (Figure 5). Obviously, as T approaches 0 K in vacuum one recovers the binding energy of 12.7 kcal/mol. The effects of entropy and temperature are readily seen in the results for 298 K, for which in agreement with expectation $\Delta G \sim -2.5$ kcal/mol in vacuum, substantially less than the 0 K limit. The latter value, nonetheless, is in the absolute values larger than the SAPT(DFT) result from ca. −1.5 kcal/mol (Table 1), but both lie within the expected uncertainty in ligand binding free energy calculations of this type (±1.5 kcal/mol).

This relatively low value of the binding Gibbs free energy explains why the CS_2 molecule leaves the host when running canonical molecular dynamics simulations at 360 K in vacuum.

dx.doi.org/10.1021/ct300546c | J. Chem. Theory Comput. 2012, 8, 4546−4555

In contrast with the vacuum result, when solvent is added (Figure 5) we obtain $\Delta G \approx -10$ kcal/mol. This explains the overall stabilizing effect of the solvent on the complex and why the CS_2 molecule will not leave the host even at temperatures close to the boiling point of the solvent.

CONCLUSIONS

The stability of H_2, N_2, CO, HCN, H_2O, CO_2, CS_2, H_2S, C_2H_2, NH_3, CH_4, CH_3CN, CH_3OH, 2-butyne, methyl halides, and noble gas atoms encapsulated by the $C_{50}H_{10}$ nanocontainer was studied using the SAPT(DFT) method. The Gibbs free energies of the encapsulation reactions were also estimated for some complexes. All complexes under study were found to be stable at $T = 0$ K, but only few of them remained stable at standard conditions. Interestingly, trying to complex $C_{50}H_{10}$ with few guests the Scott group found CS_2 one which, according to our calculations, forms the stable complex up to highest temperature of ca. 340 K.[16] For the guest molecules for which two modes of entering the container were possible, one orientation is more stable albeit the corresponding energy difference is in most close to about 1 kcal/mol. The energetically lower geometry corresponds to the methyl group situated outside the hole for guests with the methyl group or for the nitrogen (carbon) atom inside the hole for the HCN and CO molecules, respectively. This difference is less than 0.1 kcal/mol for the complex involving CO, 4.33 kcal/mol for CH_3F, 4.03 kcal/mol for CH_3I, and 3.32 kcal/mol for HCN. The estimation of the temperature at which $\Delta G = 0$ was given. The most interesting conclusion of the ΔG estimations shows that in spite of the negative energies of the interaction of the $C_{50}H_{10}$ nanotube with all guests under scrutiny only few complexes are stable and eventually could be observable. At room temperature, in addition to that with CS_2, only the complexes with the HCN, Xe, and possibly those involving CO_2, Kr, and CH_3C_2H guests are candidates for a successful complexation. Taking into account the stabilizing effect of the $CHCl_3$ solvent determined in the MD simulations for the $CS_2@C_{50}H_{10}$ complex, the application of the nanotube as a nanocontainer for the CO_2 molecules, responsible for the greenhouse effect, seems feasible. For a successful complexation of other than listed above guests, the obtainment of the next members of the series, e.g. the $C_{60}H_{10}$ open nanotube seems to be necessary.

The SAPT(DFT) results for the experimentally observed $CS_2@C_{50}H_{10}$ complex were in excellent agreement with those obtained using molecular dynamics simulations, which both predict that the complex becomes unstable at temperatures larger than ca. 350 K at 1 atm. The simulations also indicate that the $CHCl_3$ solvent stabilizes the complex.

ASSOCIATED CONTENT

Supporting Information

Models of minimized structures of all complexes under study and containing the ionization potentials, HOMO PBE energies used for the SAPT(DFT) calculations, and intermolecular guest−host vibrations for the complexes from Table 2. This material is available free of charge via the Internet at http://pubs.acs.org.

AUTHOR INFORMATION

Corresponding Author

*E-mail: dodziuk@ichf.edu.pl (H.D.); tania@chem.uw.edu.pl (T.K.).

Notes

The authors declare no competing financial interest.

ACKNOWLEDGMENTS

The authors are grateful to Prof. L. T. Scott for providing us with the results on the $C_{50}H_{10}$ nanotube prior to their publication and for his fruitful remarks to the manuscript. T.K. acknowledges the support from the National Science Centre of Poland through grant 2011/01/B/ST4/06141. E.L. and C.B. acknowledge support from the Direccion General de Investigacion Cientifica y Tecnica under Grant No. FIS2010-15502 and from the Direccion General de Universidades e Investigacion de la Comunidad de Madrid under Grant No. S2009/ESP/1691, Program MODELICO-CM.

REFERENCES

(1) Dodziuk, H. In *Mathematics and Topology of Fullerenes*; Graovac, A., Ori, O., Cataldo, F., Eds.; Springer: Hamburg, 2011; pp 117−151.
(2) Schur, D. V.; Zaginaichenko, S. Y.; Savenko, A. F.; Bogolepov, V. A.; Anikina, N. S.; Zolotarenko, A. D.; Matysina, Z. A.; Veziroglu, T. N.; Skryabina, N. E. *Int. J. Hydrogen Energy* **2011**, *36*, 1143−1151.
(3) Turker, L.; Gümüs, S. In *Handbook of Nanophysics: Clusters and Fullerenes*; Sattler, K. D., Ed.; RCR Press: Boca Raton, 2011; Vol. 2, Chapter 33-1.
(4) Yoshida, Z.-I.; Dogane, I.; Ikehira, H.; Endo, T. *Chem. Phys. Lett.* **1993**, *201*, 481−484.
(5) Suyetin, M. V.; Vakhrushev, A. V. *J. Phys. Chem. C* **2011**, *115*, 5485−5491.
(6) Kruger, A. In *Strained Hydrocarbons. Beyond van't Hoff and Le Bel Hypothesis*; Dodziuk, H., Ed.; Wiley-VCH: Weinheim, 2009; pp 335−373.
(7) Cassell, A. M.; Raymakers, J. A.; Kong, J.; Dai, H. *J. Phys. Chem. B* **1999**, *103*, 6484−6492.
(8) Journet, C.; Maser, W. K.; Bernier, P.; Loiseau, A.; la Chapelle, M. L.; Lefrant, S.; Deniard, P.; Leek, R.; Fischer, J. E. *Nature* **1997**, *388*, 756−758.
(9) Maser, W. K.; Munoz, E.; Benito, A. M.; Martinez, M. T.; de la Fuente, G. F.; Maniette, Y.; Anglaret, E.; Sauvajol, J.-L. *Chem. Phys. Lett.* **1998**, *292*, 587−593.
(10) Toth, G.; Maklin, J.; Halonen, N.; Palosaari, J.; Juuti, J.; Jantunen, H.; Kordas, K.; Sawyer, W. G.; Vajtai, R.; Ajayan, P. M. *Adv. Mater.* **2009**, *21*, 1−5.
(11) Dodziuk, H.; Dolgonos, G. *Chem. Phys. Lett.* **2002**, *356*, 79−83.
(12) Gong, K.; Du, F.; Xia, Z.; Durstock, M. *Science* **2009**, *323*, 760−764.
(13) Frank, B.; Blume, R.; Rinaldi, A.; Trunschke, A.; Schlögl, R. *Angew. Chem., Int. Ed.* **2011**, *50*, 10226−10230.
(14) Zhang, J.; Liu, X.; Blume, R.; Zhang, A.; Schlögl, R.; Su, D. S. *Science* **2008**, *322*, 73−77.
(15) Yoshimoto, S.; Tsutsumi, E.; Honda, Y.; Murata, Y.; Murata, M.; Komatsu, K.; Ito, O.; Itaya, K. *Angew. Chem., Int. Ed.* **2004**, *43*, 3044−3047.
(16) Scott, L. T.; Jackson, E. A.; Zhang, Q.; Steinberg, B. D.; Bancu, M.; Li, B. *J. Am. Chem. Soc.* **2011**, *134*, 107−110.
(17) Korona, T.; Dodziuk, H. *J. Chem. Theory Comp.* **2011**, *7*, 1476−1483 ; doi: DOI: 10.1021/ct200111a.
(18) Dodziuk, H. *J. Nanosci. Nanotechnol.* **2007**, *7*, 1102−1110.
(19) Jeziorski, B.; Moszynski, R.; Szalewicz, K. *Chem. Rev.* **1994**, *94*, 1887−1930.
(20) Szalewicz, K.; Patkowski, K.; Jeziorski, B. *Struct. Bonding (Berlin)* **2005**, *116*, 43−117.
(21) Szalewicz, K.; Jeziorski, B. In *Molecular Interactions - from van der Waals to Strongly Bound Complexes*; Schreiner, S., Ed.; Wiley: New York, 1997; pp 3−43.
(22) Hobza, P.; Selzle, H. L.; Schlag, E. W. *J. Phys. Chem.* **1996**, *100*, 18790−18794.

(23) Hesselmann, A.; Korona, T. *Phys. Chem. Chem. Phys.* **2011**, *13*, 732−743.
(24) Grimme, S. *J. Comput. Chem.* **2004**, *25*, 1463−1473.
(25) Grimme, S. *J. Comput. Chem.* **2006**, *27*, 1787−1799.
(26) Grimme, S.; Parac, M. *ChemPhysChem* **2003**, *3*, 292−295.
(27) Jeziorska, M.; Jeziorski, B.; Cizek, J. *Int. J. Quantum Chem.* **1987**, *32*, 149−164.
(28) Moszynski, R.; Heijmen, T. G. A.; Jeziorski, B. *Mol. Phys.* **1996**, *88*, 741−758.
(29) Williams, H. L.; Chabalowski, C. F. *J. Phys. Chem. A* **2001**, *105*, 646−659.
(30) Jansen, G.; Hesselmann, A. *J. Phys. Chem. A* **2001**, *105*, 11158−11158.
(31) Misquitta, A. J.; Jeziorski, B.; Szalewicz, K. *Phys. Rev. Lett.* **2003**, *91*, 033201.
(32) Misquitta, A. J.; Podeszwa, R.; Jeziorski, B.; Szalewicz, K. *J. Chem. Phys.* **2005**, *123*, 214103.
(33) Misquitta, A. J.; Szalewicz, K. *Chem. Phys. Lett.* **2005**, *357*, 301−306.
(34) Hesselmann, A.; Jansen, G. *Chem. Phys. Lett.* **2002**, *357*, 464−470.
(35) Hesselmann, A.; Jansen, G. *Chem. Phys. Lett.* **2002**, *362*, 319−325.
(36) Hesselmann, A.; Jansen, G. *Chem. Phys. Lett.* **2003**, *367*, 778−784.
(37) Hesselmann, A.; Jansen, G. *Phys. Chem. Chem. Phys.* **2003**, *5*, 5010−514.
(38) Dunlap, B. I.; Connolly, J. W. D.; Sabin, J. R. *J. Chem. Phys.* **1979**, *71*, 4993−4999.
(39) Hesselmann, A.; Jansen, G.; Schütz, M. *J. Chem. Phys.* **2005**, *122*, 054306.
(40) Hesselmann, A.; Jansen, G.; Schütz, M. *J. Am. Chem. Soc.* **2006**, *128*, 11730−11731.
(41) Podeszwa, R.; Szalewicz, K. *Chem. Phys. Lett.* **2005**, *412*, 488−493.
(42) Podeszwa, R.; Bukowski, R.; Szalewicz, K. *J. Chem. Theory Comput.* **2006**, *2*, 400−412.
(43) Podeszwa, R.; Bukowski, R.; Rice, B. M.; Szalewicz, K. *Phys. Chem. Chem. Phys.* **2007**, *9*, 5561−5569.
(44) Jenness, G. R.; Karalti, O.; Jordan, K. D. *Phys. Chem. Chem. Phys.* **2010**, *12*, 6375−6381.
(45) Korona, T.; Hesselmann, M.; Dodziuk, H. *J. Chem. Theory Comp.* **2009**, *5*, 1585−1596.
(46) Podeszwa, R.; Cencek, W.; Szalewicz, K. *J. Chem. Theory Comput.* **2012**, *8*, 1963−1969.
(47) Hohenstein, E. G.; Parrish, R. M.; Sherrill, C. D.; Turney, J. M.; Schaefer, H. F. *J. Chem. Phys.* **2011**, *135*, 174107.
(48) Korona, T.; Jeziorski, B. *J. Chem. Phys.* **2006**, *125*, 184109.
(49) Korona, T. *Phys. Chem. Chem. Phys.* **2007**, *9*, 6004−6011.
(50) Korona, T.; Jeziorski, B. *J. Chem. Phys.* **2008**, *128*, 144107.
(51) Korona, T. *Phys. Chem. Chem. Phys.* **2008**, *10*, 6509−6519.
(52) Korona, T. *J. Chem. Phys.* **2008**, *128*, 224104.
(53) Korona, T. *J. Chem. Theory Comp.* **2009**, *5*, 2663−2678.
(54) Korona, T. In *Recent Progress in Coupled Cluster Methods*; Čársky, P., Paldus, J., Pittner, J., Eds.; Springer: Dordrecht, 2010; pp 267−296.
(55) Allinger, N. L. *Adv. Phys. Org. Chem.* **1976**, *13*, 1−82.
(56) Osawa, E.; Musso, H. *Angew. Chem., Int. Ed. Engl.* **1983**, *22*, 1−12.
(57) Wang, C.; Straka, M.; Pyykko, P. *Phys. Chem. Chem. Phys.* **2010**, *12*, 6187−6203.
(58) http://www.gaussian.com/g_whitepap/thermo.htm (accessed August 2011).
(59) Slanina, Z.; Adamowicz, L.; Kobayashi, K.; Nagase, S. *Molec. Simul.* **2005**, *31*, 71−77.
(60) Fernandez-Ramos, A.; Ellingson, B. A.; Meana-Paneda, R.; Marques, J. M. C.; Truhlar, D. G. *Chem. Theor. Acc.* **2007**, *118*, 813−826.
(61) LAMMPS is a classical molecular dynamics code, and an acronym for Large-scale Atomic/Molecular Massively Parallel Simulator (see http://lammps.sandia.gov), 2010.
(62) Plimpton, S. *J. Comput. Phys.* **1995**, *117*, 1−19.
(63) Plimpton, S. J.; Thompson, A. P. *MRS Bull.* **2012**, *37*, 513−521.
(64) Jaramillo-Botero, A.; Su, J.; Qi, A.; Goddard, W. A., III *J. Comput. Chem.* **2011**, *32*, 497−512.
(65) Schlitter, J.; Swegat, W.; Mülders, T. *J. Mol. Model* **2001**, *7*, 171−177.
(66) Stuart, S. J.; Tutein, A. B.; Harrison, J. A. *J. Chem. Phys.* **2000**, *112*, 6472−6486.
(67) Brenner, D. W.; Shenderova, O. A.; Harrison, J. A.; Stuart, S. J.; Ni, B.; Sinnott, S. B. *J. Phys.: Condens. Matter* **2002**, *14*, 783−802.
(68) Ni, B.; Sinnott, S. B.; Mikulski, P. T.; Harrison, J. A. *Phys. Rev. Lett.* **2002**, *88*, 205505.
(69) Liu, H. J.; Cho, K. *Appl. Phys. Lett.* **2004**, *85*, 807−809.
(70) Kholmurodov, K.; Aru, G.; Yasuoka, K. *Nat. Sci.* **2010**, *2*, 902−910.
(71) Zhu, S. B.; Lee, J.; Robinson, G. W. *Mol. Phys.* **1988**, *65*, 65−75.
(72) Reed, A. E.; Weinstock, R. B.; Weinhold, F. *J. Chem. Phys.* **1985**, *83*, 735−746.
(73) Mata, R.; Werner, H.-J. *Mol. Phys.* **2007**, *105*, 2753−2761.
(74) Perdew, J. P.; Burke, K.; Ernzerhof, M. *Phys. Rev. Lett.* **1996**, *77*, 3865−3868.
(75) Phillips, J. M.; Hammerbacher, M. D. *Phys. Rev. B* **1984**, *29*, 5859−5864.
(76) Benjamin, I. *J. Chem. Phys.* **1995**, *103*, 2459−2471.
(77) Allen, M. P.; Tildesley, D. J. *Computer Simulation of Liquids*; Oxford University Press: Oxford, 1989.
(78) Rappe, A. K.; Casewit, C. J.; Colwell, K. S.; Goddard, W. A.; Skiff, W. M. *J. Am. Chem. Soc.* **1992**, *114*, 10024−10039.
(79) Argus, ArgusLab is a molecular modeling, graphics, and drug design program. http://www.arguslab.com (accessed 2005).
(80) Frisch, M. J.; Trucks, G. W.; Schlegel, H. B.; Scuseria, G. E.; Robb, M. A.; Cheeseman, J. R.; Montgomery, J. A., Jr.; Vreven, T.; Kudin, K. N.; Burant, J. C.; Millam, J. M.; Lyengar, S. S.; Tomasi, J.; Barone, V.; Mennucci, B.; Cossi, M.; Scalmani, G.; Rega, N.; Petersson, G. A.; Nakatsuji, H.; Hada, M.; Ehara, M.; Toyota, K.; Fukuda, R.; Hasegawa, J.; Ishida, M.; Nakajima, T.; Honda, Y.; Kitao, O.; Nakai, H.; Klene, M.; Li, X.; Knox, J. E.; Hratchian, H. P.; Cross, J. B.; Bakken, V.; Adamo, C.; Jaramillo, J.; Gomperts, R.; Stratmann, R. E.; Yazyev, O.; Austin, A. J.; Cammi, R.; Pomelli, C.; Ochterski, J. W.; Ayala, P. Y.; Morokuma, K.; Voth, G. A.; Salvador, P.; Dannenberg, J. J.; Zakrzewski, V. G.; Dapprich, S.; Daniels, A. D.; Strain, M. C.; Farkas, O.; Malick, D. K.; Rabuck, A. D.; Raghavachari, K.; Foresman, J. B.; Ortiz, J. V.; Cui, Q.; Baboul, A. G.; Clifford, S.; Cioslowski, J.; Stefanov, B. B.; Liu, G.; Liashenko, A.; Piskorz, P.; Komaromi, I.; Martin, R. L.; Fox, D. J.; Keith, T.; Al-Laham, M. A.; Peng, C. Y.; Nanayakkara, A.; Challacombe, M.; Gill, P. M. W.; Johnson, B.; Chen, W.; Wong, M. W.; Gonzalez, C.; Pople, J. A. *Gaussian 03*, revision C.02; Gaussian, Inc.: Wallingford CT, 2003.
(81) Becke, A. D. *Phys. Rev. A* **1988**, *38*, 3098−3100.
(82) Lee, C.; Yang, W.; Parr, R. G. *Phys. Rev. B* **1988**, *57*, 785−789.
(83) Becke, A. D. *J. Chem. Phys.* **1993**, *98*, 5648−5652.
(84) Hehre, W.; Ditchfield, R.; Pople, J. *J. Chem. Phys.* **1972**, *56*, 2257−2261.
(85) Werner, H. J.; Knowles, P. J.; Manby, F. R.; Schütz, M.; Celani, P.; Knizia, G.; Korona, T.; Lindh, R.; Mitrushenkov, A.; Rauhut, G.; Adler, T. B.; Amos, R. D.; Bernhardsson, A.; Berning, A.; Cooper, D. L.; Deegan, M. J. O.; Dobbyn, A. J.; Eckert, F.; Goll, E.; Hampel, C.; A., H.; Hetzer, G.; Hrenar, T.; Jansen, G.; Köppl, C.; Liu, Y.; Lloyd, A. W.; Mata, R. A.; May, A. J.; McNicholas, S. J.; Meyer, W.; Mura, M. E.; Nicklass, A.; Palmieri, P.; Pflüger, K.; Pitzer, R.; Reiher, M.; Shizoaki, T.; Stoll, H.; Stone, A. J.; Tarroni, R.; Thorsteinsson, T.; Wang, M.; Wolf, A. *MOLPRO*, version 2010.2, 2010.
(86) Grüning, M.; Gritsenko, O. V.; van Gisergen, S. J. A.; Baerends, E. J. *J. Chem. Phys.* **2001**, *114*, 652−660.
(87) Computational Chemistry Comparison and Benchmark DataBase. http://cccbdb.nist.gov (accessed August 2011).

(88) Godbout, N.; Salahub, D. R.; Andzelm, J.; Wimmer, E. *Can. J. Chem.* **1992**, *70*, 560−571.
(89) Schafer, A.; Huber, C.; Ahlrichs, R. *J. Chem. Phys.* **1994**, *100*, 5829−5835.
(90) Dunning, T. H., Jr.; Hay, P. J. In *Methods of Electronic Structure Theory*; Schaefer, H. F., III, Ed.; Plenum Press, 1977; *Vol. 2*.
(91) Kendall, R. A.; Dunning, J., T. H.; Harrison, R. J. *J. Chem. Phys.* **1992**, *96*, 6796−6806.
(92) Peterson, K. A.; Yousaf, K. E. *J. Chem. Phys.* **2010**, *133*, 174116.
(93) Peterson, K. A.; Shepler, B. C.; Figgen, D.; Stoll, H. *J. Phys. Chem. A* **2006**, *110*, 13877−13883.
(94) Weigend, F.; Häser, M.; Patzelt, H.; Ahlrichs, R. *Chem. Phys. Lett.* **1998**, *294*, 143−152.
(95) Weigend, F. *J. Comput. Chem.* **2008**, *29*, 167−175.